

RPM ESTIMATION THROUGH RFID TECHNOLOGY

BS Electrical Engineering

Session: 2019 - 20

By:

| | |
|-----------------------|----------|
| Irtaza Shahid | 20100181 |
| Waleed Akbar | 20100055 |
| Muhammad Farid Haroon | 20100155 |

Supervised by:

Dr. Muhammad Tahir,
Assistant Professor, EE

Co-Supervised by:

Dr. Momin Ayyub Uppal,
Associate Professor, EE



Department of Electrical Engineering
Lahore University of Management Sciences

Abstract

With the rapid development and advancements in modern industry and its technology, rotating machinery is one of the most essential equipment in the world we know today. Fault diagnosis of rotating machinery plays a significant role in the reliability and safety of modern industrial systems. Each year, numerous industrial machines experience a 'downtime' due to the necessary maintenance checks, which costs industries billions in revenue and affect their production. If only the industries could identify the fault (if any) in their operating machinery non-invasively, the unnecessary 'downtime' could be avoided. One possible way to achieve this goal is to continuously monitor the revolution per minute (RPM) of the machine to capture any deviation from the norm and act before things get catastrophic. Deploying radio frequency identification (RFID) technology for continuous RPM monitoring could be an effective and feasible solution to the problem. The backscattered signal from an RFID tag contains valuable information that can be processed and manipulated. Perhaps the biggest advantage that RFID technology has to offer is the ability to work without a line of sight from tag to reader. Given the extent of the applicability of the RFID technology, our objective is to investigate the potential of using various signal processing techniques to extract and process the information from the backscattered RFID signal to effectively measure and monitor the RPM of the machine.

Acknowledgments

The authors wish to express sincere appreciation to Dr. Muhammad Tahir and Dr. Momin Uppal for their dedicated supervision during the course of this senior year project and in the preparation of this manuscript.

Originality Certificate

“We the undersigned certify that this submission is the original work of members of the group and meets the Faculty's Expectations of Originality”:

1. Irtaza Shahid [2020-10-0181]

Signed: _____ 20100181@lums.edu.pk

2. Waleed Akbar [2020-10-0055]

Signed: _____ 20100055@lums.edu.pk

3. Muhammad Farid Haroon [2020-10-0155]

Signed: _____ 20100155@lums.edu.pk

Advisor

Dr. Muhammad Tahir

tahir@lums.edu.pk

Co-Advisor(s)

Dr. Momin Ayyub Uppal

momin.uppal@lums.edu.pk

Contents

| | | |
|----------|--|-----------|
| 4.2 | Experimental Procedure: | 17 |
| 4.3 | Implementation Results: | 17 |
| 5 | Software Implementation | 19 |
| 5.1 | Reconstructing Vibration Signal | 19 |
| 5.1.1 | Compressive Sensing: | 19 |
| 5.1.1.1 | Problem Formulation: | 19 |
| 5.1.1.2 | Implementation: | 21 |
| 5.1.1.3 | Effect of Noise on recovery: | 23 |
| 5.2 | Measuring Vibrational Period | 23 |
| 5.2.1 | Fourier Transform: | 23 |
| 5.2.2 | Finding Time Period Through Correlation Method: | 24 |
| 5.3 | Experimentation | 25 |
| 5.4 | Error Analysis | 28 |
| 6 | Conclusion, Future Recommendations, And Cost Analysis | 29 |
| 6.1 | Conclusion and Future Recommendations | 29 |
| 6.2 | Cost Analysis | 30 |

List of Figures

| | | |
|-----|--|----|
| 1.1 | The general block diagram for machine health prediction | 2 |
| 1.2 | Timeline of the project | 3 |
| 2.1 | The difference that fractions of availability in industrial machinery . | 5 |
| 2.2 | Condition Based Monitoring. | 8 |
| 2.3 | How condition-based maintenance helps predict and prevent unplan. | 8 |
| 2.4 | Passive RFID Systems Overview [1] | 9 |
| 2.5 | Gen 2 Protocol (Courtesy of EPCglobal) | 9 |
| 2.6 | Inventory round between tag and reader. | 9 |
| 3.1 | System level design | 11 |
| 4.1 | Passive RFID Tag | 14 |
| 4.2 | Inventory Round | 15 |
| 4.3 | EPC, phase, and RSSI | 18 |
| 5.1 | Reconstructed signal 1 | 22 |
| 5.2 | Reconstructed signal 2 | 22 |
| 5.3 | Effect of noise on error | 23 |
| 5.4 | The correlation of a periodic signal with respect to lag | 25 |
| 5.5 | The reconstructed vibration signal of an induction motor rotating at 2402 RPM and its correlation with respect to lag | 26 |
| 5.6 | The reconstructed vibration signal of an induction motor rotating at 1820 RPM and its correlation with respect to lag | 26 |
| 5.7 | The reconstructed vibration signal of an induction motor rotating at 1365 RPM and its correlation with respect to lag | 27 |
| 5.8 | The reconstructed vibration signal of an pedestal fan rotating at 1034 RPM and its correlation with respect to lag | 27 |
| 5.9 | The mean, minimum, and maximum error in a measurement with respect to the corresponding RPMs | 28 |

List of Tables

| | |
|--|----|
| 2.1 Advantages and disadvantages of various techniques for RPM measurement | 10 |
| 6.1 Cost Analysis | 30 |

Chapter 1

Introduction

1.1 Motivation

The project aims to explore the potential of using radio frequency Identification (RFID) technology and signal processing in conjunction in the area of condition-based maintenance of industrial machinery through Revolutions Per Minute (RPM) monitoring. We have observed that many industries are forced to shut down their entire plants to carry out the necessary maintenance checks regardless of the machine health and this costs them millions in revenue [2]. If somehow industries, particularly those that rely on rotatory machines, could continuously monitor the important machine's health indicators, such as RPM, they may well be able to avoid the unnecessary downtimes by taking timely steps, and could significantly raise the plant efficiency, productivity and ensure its safety. To achieve this goal, it is essential to develop a non-invasive and non-line-of-sight technique to monitor the RPM of a machine consistently and report any irregularities.

1.2 Problem Statement

We aim to investigate the prospects of developing a non-invasive, non-line-of-sight solution for monitoring the RPM of a rotatory machine using the RFID technology in conjunction with the signal processing.

1.3 General Block Diagram

The Fig1.1 shows that our project comprises of various stages. We use a lab motor to perform the experiments for data collection. RFID tagged motor operates in

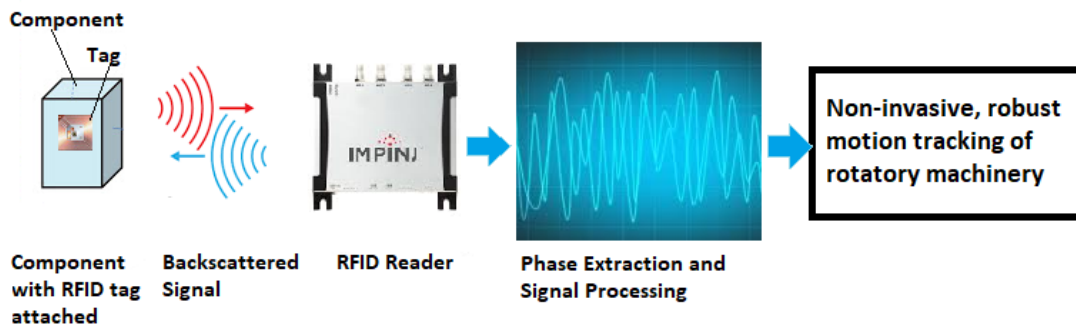


FIGURE 1.1: The general block diagram for machine health prediction

the vicinity of an RFID reader. The RFID reader communicates with the tag through the electronic product code (EPC) class 1 Gen 2 protocol, and RFID tag responds to the reader's signal by backscattering the incident radio frequency (RF) wave. The reader demodulates the received signal, and this demodulation allows the reader to measure the phase of the received signal. Once we have the phase, we perform various signal processing techniques to process the information embedded in the phase. Since the rotatory motion is periodic, the phase of the backscatter signal captures that periodic nature of the motion through continuous communication between the tag and the reader.

1.4 Social Benefits And Relevance

The industrial machinery in today's industrial units must be powered-off after a specified duration of time to carry out, possibly unnecessary, maintenance checks that can last for a few weeks or even months. This results in potentially valuable time to go to waste had the machine already been in full health. Our project aims to develop a system that can continuously monitor the RPM of the industrial machines, which is a critical indicator of a rotatory machine's health, so that the maintenance can be conducted only when a potential fault has been detected. This will significantly increase industrial plant efficiency and productivity to benefit the country's economy and trade. Apart from that, this will ensure that no faulty machine is in operation and thus, will contribute to the safety of the workers and the industry itself.

1.5 Goals and Objectives

Our goal is to come up with a system that will non-invasively track the RPM of the rotatory machines using RFID technology and signal processing to help industries

in constant monitoring of machine's operation. Our project's objectives comprise of the following:

- Extraction of the time-varying phase of the backscattered signal from the RFID tags using an RFID reader.
- Since the periodic phase signal is sparse in the Fourier domain, it allows us to reconstruct the signal through compressed sensing techniques.
- The reconstructed signal is then used to estimate the RPM through auto-correlation.

1.6 Outcomes and Deliverables

The deliverables of our project will comprise of:

- Identification of Ultra High Frequency (UHF) RFID tags using IMPINJ R420 reader.
- Phase extraction from the backscattered signal from the RFID tags along with the timestamp.
- Preprocessing of the raw phase signal.
- Reconstruction algorithm for a non-uniformly sampled periodic signal.
- Estimation of RPM through reconstructed signal.

1.7 Timelines and the distribution of work

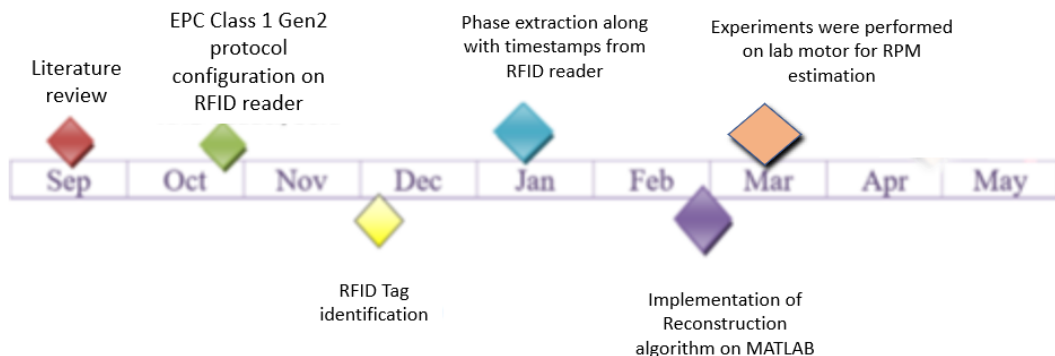


FIGURE 1.2: Timeline of the project

By the end of September 2019, we were done with the literature review. During October and November, we learned the reader operation and integrated the reader's hardware and software. Once we were equipped with the essential knowledge needed to operate the reader, we did the tag reading and identification. Tag responds to an incident signal from the reader and sends its electronic product code (EPC) by backscattering the incident radio frequency wave. We did the multiple tags identification in the vicinity of the reader. Next phase in our project was the phase extraction along with the timestamps from the reader. This was the most crucial stage of our project as all the information lies in the phase of the received signal. After the extraction of phase along with timestamps, we moved toward the implementation of the reconstruction algorithm. By the mid of March, we were testing the algorithm on the data gathered from the lab DC motor and we were correctly estimating the RPM. Fig1.2 shows the general summary of the timeline of our project.

Chapter 2

Background

2.1 Literature Review

In most industries, downtime is the greatest source of loss in production time. Downtime can occur as a result from hardware failure, software failure, maintenance checks, overload, security breach etc. From 2014 to 2015, the average cost per hour of downtime across all businesses reportedly increased by 60% from \$164,000 to \$260,000 [3]. Hence, every fraction of availability of a machine is extremely valuable to industries and businesses as the Fig2.1 shows the huge difference between 99% availability and the rest [4].

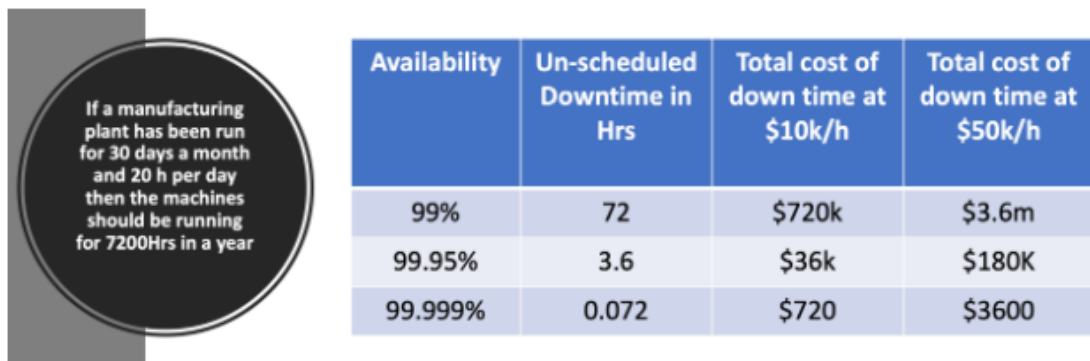


FIGURE 2.1: The difference that fractions of availability in industrial machinery

Mark Homer, vice-president of global customer transformation at ServiceMax, said: "Outages tend to go unnoticed. The survey found that 70% of companies have a lack of awareness about when their assets need to be maintained" [5][6]. Over the past 3 years, 82% of companies have experienced more than one unplanned downtime outages and cost an average of \$2 million [6].

Industries usually must tolerate the downtimes of their machinery by attempting

to identify and solve the fault as rapidly as possible to continue production. However, machine and equipment failure continue to occur in manufacturing facilities and methods such as risk-based inspection (RBI), failure elimination, root cause analysis, failure mode and effects analysis (FMEA) and reliability-centered maintenance (RCM) are deployed [4]. Though these costly methods are great on their own in reducing unplanned downtime, they do not help to prevent nor predict it. The most common type of equipment in mechanical industries is rotatory machinery. It is a major and critical component of many mechanical systems in industrial plants, air and ground transportation vehicles, and in many other applications [7]. Hence, it is not surprising that fault detection of rotatory machinery is of growing importance as the cost of both production and maintenance is extremely critical. Apart from this, due to rapidly progressing technology, the design of rotatory machinery is becoming increasingly complex. So, machinery condition monitoring strategies need to become more advanced as well to cope up with the physical burdens being placed on the individual components of a machine [8].

To evaluate condition of an equipment, vibration analysis needs to be done effectively. For rotatory machinery, when looking at vibrational signals, multiples of rotating speed or RPM plays a crucial role in determining machine health. Vibrational frequencies at multiples of RPM correspond with the number of components in a specific part, such as the number of balls in a bearing [9]. Hence, in an equipment with rotating speed of 1000 RPM, a frequency peak at 50000 RPM prompts us to look for a part in the machine containing $50000/1000 = 50$ components. Apart from this, if the amplitude of these peaks at higher multiples of rotating speed increases significantly, it may indicate developing problems like a high fan blade passing a fixed protrusion or a damaged impeller blade for example [9]. However, care must be taken so that we know what the true running speed of our motor is, because the nameplate speed is usually the manufacturer's average speed for a specific design. Hence, accurate measurement of RPM is crucial in this kind of analysis.

Another way to detect faults using RPM is through the rotor-bar or slot-passing frequency. For example, a 60 horsepower (hp) motor with 30 rotor bars that operate at 1800 RPM would have a bar-passing frequency of $(30 \times 1800 = 54000)$ 54000 RPM. This is because defective motor bars usually increase the amplitude of the bar-passing frequency for the motor [9].

There are also some specific existing problems that are already known to be diagnosed using RPM measurements. Misalignment, looseness, rubbing, imbalance and belt defects are diagnosed due to frequency peaks between 1.5 to 2.5 times the base RPM [10]. Late-stage bearing fault harmonics and electrical issues are

diagnosed generally due to frequency peaks between 4.5 to 50 times the base [10]. Other faulty parts that can be diagnosed may include impeller vanes, rotor bars or stator slots, fan blades or a combination thereof [9]. Hence, RPM is a critical element in indication and diagnosis of various machine faults.

Our project aims to develop a system that continuously monitors the RPM in industrial setup where multiple rotatory machines operate simultaneously. Due to the numerous machines, industrial environments are mostly occluded, and it is essential to develop a system that will enable non-invasive and non-line-of-sight uninterrupted monitoring of RPM. Such system will allow for condition-based maintenance (CBM) to decide what maintenance needs to be done to take timely corrective action. Maintenance costs can reduce by as much as four-fold by minimizing planned and unplanned downtime using predictive capability [11].

CBM is a maintenance strategy that monitors the actual health of an asset and dictates that maintenance should only be performed when certain indicators such as RPM show sign of decreasing performance or upcoming failure [12]. Fig2.2 shows a block diagram of the CBM process [13]. CBM can be applied to both mission critical and non-mission critical equipment. Hence, CBM allows for improved equipment reliability, minimized unscheduled downtime, minimized time spent on maintenance, minimizes requirement for emergency spare parts, improves worker safety, reduces the chances of collateral damage to the system etc. [12]. Fig2.3 shows some of the statistical improvements that CBM brings while preventing unplanned downtime [14]. Apart from this, an RFID implementation may be considered ideal for applying CBM strategy as a single RFID IMPINJ R420 reader system can be extended to 32 antennas with antenna hubs [15], while reading up to 1100 tags per second which could potentially monitor the RPM of 1100 occluded machines per second.

To achieve this, we have used passive UHF RFID technology. A passive RFID system primarily consists of two parts, the RFID reader and an RFID tag as shown in Fig2.4. The reader transmits high power continuous RF waves that power the chip in the tag. The tag replies to the reader by reflecting the RF wave using ON-OFF keying. Each RFID tag has a unique Electronic Product code (EPC) associated with it. Hence, each tagged machine will have a unique ID, and the system will be able to distinguish the RPM signal in an industrial setting.

In 2004, the EPC global Class 1 Generation 2 (Gen2) standard UHF RFID was introduced [16][17] as shown in Fig2.5.

Ever since, passive UHF RFID tags have slowly gained popularity in various uses and scenarios.

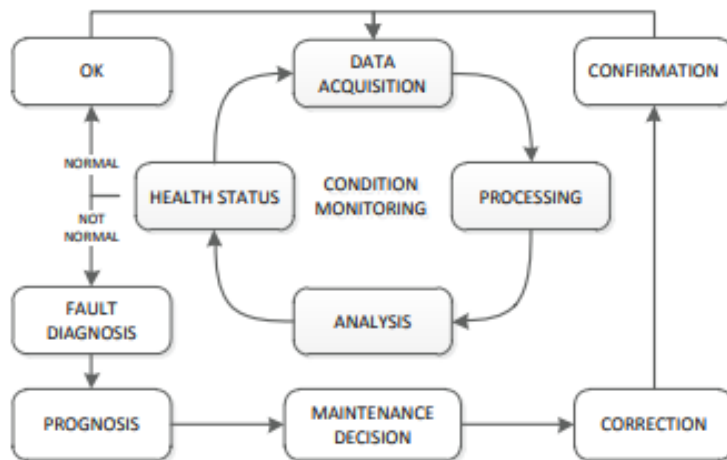
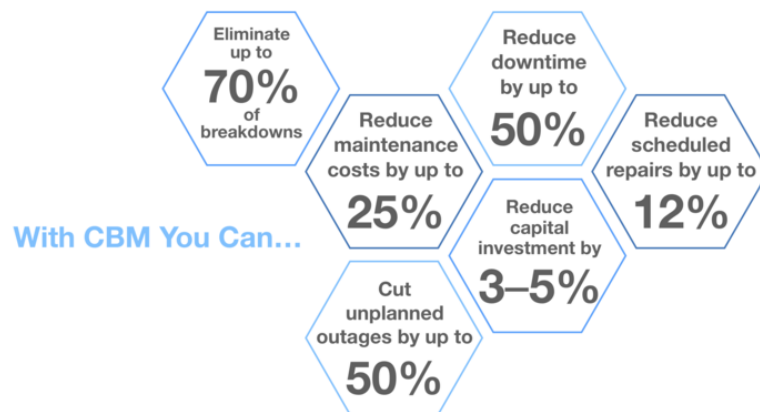


FIGURE 2.2: Condition Based Monitoring.

How Condition-Based Maintenance Helps Predict And Prevent Unplanned Downtime



Source: IBM Internet of Things: "Improving Operations With Predictive Maintenance"

FIGURE 2.3: How condition-based maintenance helps predict and prevent un-plan.

Fig2.6 from [18] represents an entire inventory round of a tag and reader communication. Reader initiates the communication by sending a query command which marks the beginning of an inventory round. After sending the query command, the reader stays quiet and waits for the tag to respond. Tag responds by backscattering the continuous radio frequency wave and it sends a random 16-digit number (RN16) using FM0 modulation. The reader receives this number and tries to decode it. The reader then sends acknowledgment command which includes the successfully decoded RN16. Tag verifies the received RN16 against the number that it originally sent and if both number matches, tag responds by sending the EPC code which is unique. If, however, received RN16 does not match the sent

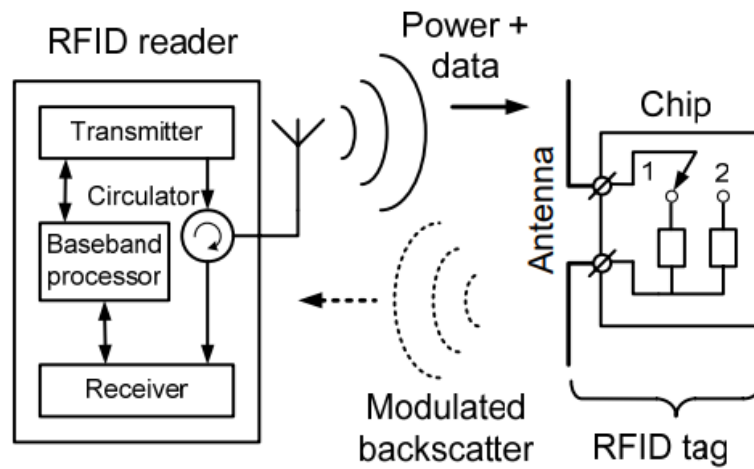


FIGURE 2.4: Passive RFID Systems Overview [1]

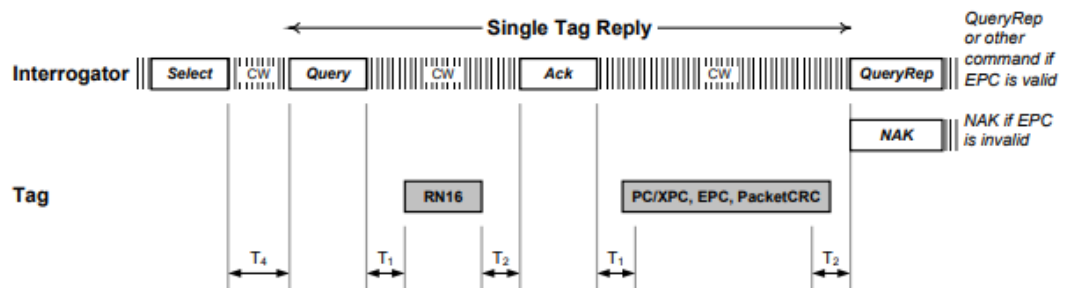


FIGURE 2.5: Gen 2 Protocol (Courtesy of EPCglobal)

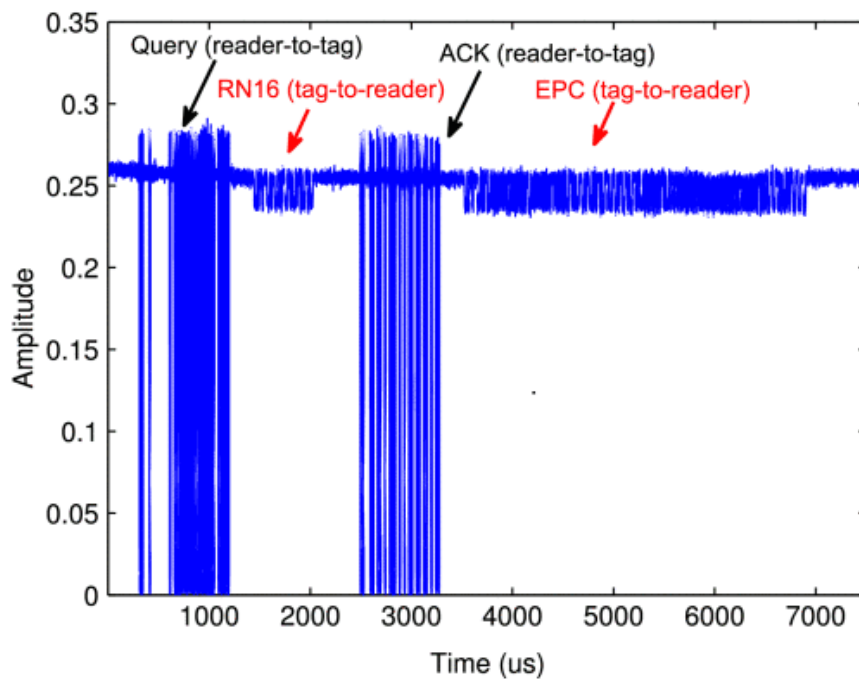


FIGURE 2.6: Inventory round between tag and reader.

RN16 then the tag simply discards the reader request.

In our work we aim to exploit the information embedded in the backscattered signal of Commercial Off-The Shelf (COFTS) RFID tags using a RFID reader using the standard in [16]. Together with IMPINJ’s libraries such as low-level reader protocol (LLRP) [19] and compressive reading techniques, the phase from backscattered signals has allowed to achieved sub-millisecond period accuracy from low-frequency reading of tags by inspecting mechanical vibration [20]. The work in [20] has been extended to a robust spinning sensing system by deploying two RFID tags on a single rotatory machine in [21]. We intend to apply a modified spinning sensing system to that in [21] to industrial machinery for non-invasive and non-line of sight RPM tracking using compressive sensing to take advantage of the periodicity and sparsity of the phase signal.

Meanwhile, other spinning sensing techniques do exist such as the use of accelerators, that require mechanical sensor deployment to capture the force induced on the instrument. This uses the fact that centrifugal force is dependent upon the speed of the object [22]. However, this requires a contact between the equipment and instrument. Apart from this, tachometers use infrared/laser to determine the rotation speed by measuring the rate at which the beam is reflected back. Also, high-frame-rate cameras capture the high-speed rotations as well. A general framework for image-based analysis of repeating motions is presented by Seitz and Dyer in [23]. But both the tachometer and camera require a line-of-sight to be deployed. Table 2.1 summarizes these comparisons.

TABLE 2.1: Advantages and disadvantages of various techniques for RPM measurement

| Technique | Contactless | Price | NLOS | Deployment | Accuracy (%) |
|----------------|-------------|--------|---------------|------------|--------------|
| Accelerator | No | Medial | Not Supported | Difficult | High |
| Infrared/laser | Yes | High | Not Supported | Difficult | Low |
| Camera | Yes | High | Not Supported | Difficult | Medium |
| Our Project | Yes | Low | Supported | Easy | High |

Chapter 3

Methodology and Tools

3.1 System Level Design

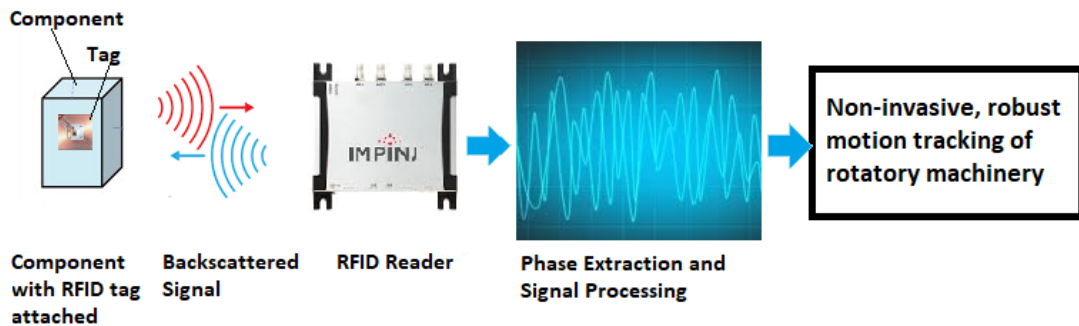


FIGURE 3.1: System level design

- **Motors (Components):** To be tested upon by attaching the RFID tag. Motor operates at different speeds.
- **RFID Reader:** It transmits UHF electromagnetic (EM) waves to the tag attached to the motor. The tag then backscatters this wave and encodes information in it for the reader to decode it.
- **Signal Processing:** The information about phase and doppler frequency is then extracted from the decoded backscatter signal from the reader along with the timestamps. The periodic phase signal is recovered from non-uniformly sampled phase data through compressive sensing techniques. Then the periodic recovered phase signal is used along with autocorrelation to determine the RPM of the component under observation.

3.2 Tools/Instruments

3.2.1 Simulation Software Packages

- Visual Studio in C# for using Low-Level Reader Protocol (LLRP) libraries.
- Item Test for testing reader.
- MATLAB for signal processing and algorithm implementation.
- Windows.

3.2.2 Hardware Instruments

- x1 IMPINJ R420 reader.
- x4 UHF Circular Polarized Antennas with 9dBm gain.
- COTS UHF RFID tags.
- 1 Computer with at least 8GB RAM

Chapter 4

Project Implementation

4.1 Hardware Setup

4.1.1 RFID Tags:

There are primarily two types of RFID tags: Active tags and Passive tags. As the name suggests, the active RFID tags contain an onboard battery as a power supply, whereas a passive RFID tag does not contain a battery and instead, relies on the electromagnetic energy transmitted from an RFID reader. The battery-less nature of passive RFID tags makes them cheap and removes the hassle of changing batteries, hence making them feasible for our application.

Fig4.1 shows the structure of a typical passive RFID tag. Integrated antenna is primarily responsible for sending and receiving signals from the reader, and microchip contains the information such as EPC. Passive RFID tags use the three main frequencies to transmit information: 125 – 134 KHz, also known as Low Frequency (LF), 13.56 MHz, also known as High Frequency (HF) and Near-Field Communication (NFC), and 865 – 960 MHz, also known as Ultra High Frequency (UHF) [24]. The frequency used affects the tag's range. For our application, we are using UHF tags since they have the largest range.

4.1.2 RFID Reader:

RFID reader, sometimes also known as interrogator, manage tag populations using the three basic operations [25]. Each of these operations comprises one or more commands. The operations are defined as follows:

- **Select:** The process by which an interrogator selects a tag population for inventory and access. Interrogators may use one or more Select commands to select a tag population prior to inventory.

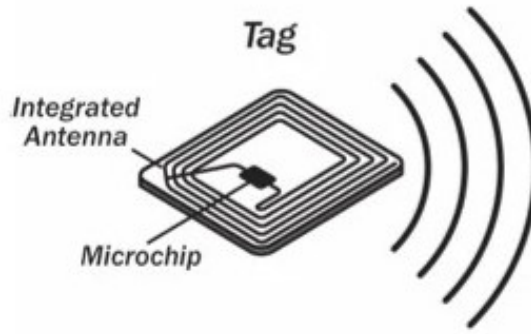


FIGURE 4.1: Passive RFID Tag

- **Inventory:** The process by which an Interrogator identifies tags. An interrogator begins an inventory round by transmitting a Query command in one of four sessions. One or more Tags may reply. The interrogator detects a single tag reply and requests the EPC and cyclical redundancy check (CRC)-16 from the tag. An inventory round operates in only one session at a time.
- **Access:** The process by which an interrogator transacts with (that is, reads from or writes to) individual tags. An individual tag must be uniquely identified prior to access.

Fig4.2 2 depicts a typical inventory round of EPC class-1 Gen2 UHF RFID protocol. The interrogator initiates an inventory round by issuing a Query command to which Tag responds with a random number of 16 bits (RN-16). The reader decodes the RN-16 and sends the acknowledge command which includes the decoded RN-16. If the decoded RN-16 is correct, the tag responds with the EPC, and if the RN-16 is invalid, the reader command is discarded.

The entire communication between a tag and the reader happens through electromagnetic waves and the phase of these waves could convey us crucial information about the tagged object. Fortunately, many commercial readers do provide us the phase associated with the decoded EPC.

4.1.2.1 Low-Level-Reader-Protocol (LLRP) and Phase Extraction:

In our experiments, we have used the IMPINJ Speedway R420 reader. Among other things, IMPINJ readers support LLRP Toolkit (LTK) [26], which provides Microsoft .NET, Java, C++, and C libraries for development of applications requiring low level control of IMPINJ Speedway RFID readers and gateways using the EPCglobal LLRP v1.0.1. These LTK libraries allow us to access the low-level data such as RF phase angle, doppler frequency and peak RSSI via LLRP. The “Hello World” LLRP application code is available at [27]. In order to extract the

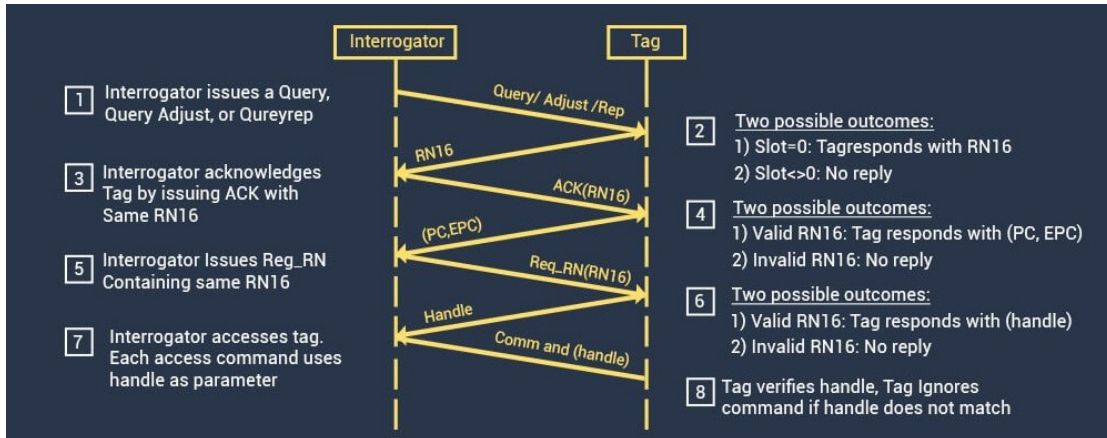


FIGURE 4.2: Inventory Round

phase and RSSI associated with an EPC, we need to enable some custom IMPINJ extensions and these details can be found at [28].

In addition to the LTK libraries, IMPINJ readers also support ItemTest software [25]. ItemTest is a simple, easy-to-use, Windows-compatible application that can be used to evaluate the functionality of an IMPINJ reader. Although ItemTest does not give us the phase, it does, however, gives us EPC, RSSI, timestamp, and allows us to change the EPC of the tags. This application also allows us to change the inventory round settings. In summary, this application is helpful in understanding the protocol and in getting started with the reader.

4.1.2.2 Extracted phase and its limitation:

Since IMPINJ's RFID reader uses 12 bits analogue to digital converter, the raw value of phase is between 0 and 4095. In order to get the phase in radians, the raw value is divided by 4096 and multiplied by 2π . According to IMPINJ's low level user data support [29], a reader might employ open-loop estimation techniques such as preamble correlation or closed-loop estimation for acquiring and/or tracking carrier phase. In all cases the phase estimate must be derived from the received signal and the estimate will be a function of the Signal-to-Noise-Ratio (SNR). The more noise energy within the receiver bandwidth, the greater the phase standard deviation. Thermal noise from the reader receiver is always present but other noise sources, such as external interference, can also affect the reported RF phase. In addition to this environmental affect, the inherent signal processing of Speedway Revolution reader introduces an ambiguity of π radians in the reported phase such that the reported phase can be the true phase (θ) or the true phase plus π radians ($\theta + \pi$).

In order to work around this ambiguity, which can severely affect the results of our experiments, we transformed our phase signal from $\theta(t)$ to $\sin(2\theta(t))$. It is

easy to see that this resolves the ambiguity of phase and this transformed signal is periodic with the same period as that of $\theta(t)$: Let T be the period of $\theta(t)$

$$\theta(t + T) = \theta(t)$$

$$\sin(2\theta(t + T)) = \sin(2\theta(t))$$

$$\sin(2(\theta(t + T) \pm \pi)) = \sin(2\theta(t) \pm 2\pi)$$

since sine is periodic with 2π so:

$$\sin(2(\theta(t + T) \pm \pi)) = \sin(2\theta(t))$$

4.1.2.3 EPC Gen2 Search Modes and Session:

IMPINJ RFID readers and gateways can be configured using many settings to handle various use-cases. Two important configuration settings are "Session" and "Search Mode". IMPINJ software (e.g. ItemTest) and libraries (e.g. LTK) allow us to change these settings [30].

Sessions and Search Modes:

The EPC GEN 2 standard allows for inventorying up to four sessions; these sessions serve two purposes:

- Determines when a tag will respond to a query from the reader.
- Allows tags to maintain independent states when communicating with multiple readers at the same time.

As defined in the EPC Gen2 Standard, the session is an inventory process comprised of the reader and an associated tag population. The IMPINJ reader chooses one of four sessions and inventories tags within that session.

The EPC GEN 2 compliant tag has two states for each session represented by Session Inventory Flags, 'A' and 'B'. The tags will always power up into the 'A' state for each session. The IMPINJ reader controls when the tag will go from 'A' to 'B' state. Although the IMPINJ reader can control when the tag is moved back to the 'A' state, it is commonly controlled by what we call the tag's persistence. When the IMPINJ reader inventories a tag, the session flag state is changed from 'A' to 'B' - how long the tag stays in the 'B' state before reverting back to the 'A' state is called "persistence". There are currently five search modes available on the IMPINJ readers:

- Dual Target

- Single Target
- Single Target with Suppression (TagFocus)
- Dual Target Select B \rightarrow A
- Single Target Reset

Each of the above search mode has its own uses, however the mode that suited our application was dual target because it allows fast reading of tags i.e. high sampling rate. In Dual Target the IMPINJ reader

- Reads 'A' tags one at a time and moves them into the 'B' state.
- Reads 'B' tags one at a time and moves them into the 'A' state.
- Repeats the above activities over and over.

In this search mode, the session has no influence as the IMPINJ reader will immediately 'push' tags back into the 'A' state. Dual target suits our application since our environment is dynamic and in dynamic environments, Dual Target can be good at detecting when a tag enters, stays, and leaves the Field of View of the antenna.

4.2 Experimental Procedure:

We tagged the rotatory machines (e.g. pedestal fans, lab DC-motors) and placed the circularly polarised antenna at a distance. The reader collected the values of phase from the rotating machine in dual-target search mode and the acquired values of phase, along with the timestamp was passed to the Matlab to estimate the RPM through signal processing.

4.3 Implementation Results:

Fig4.3 shows the screenshot of one of our experiment, capturing the EPC, phase values, and RSSI. The experiment was performed when the machine was still, and this can be seen through relatively constant values of phase. The dual-target mode enabled us to achieve the average sampling rate of around 140 tag reads per second. The figure also shows that the RSSI is constant over the duration of the experiment.

Chapter 5

Software Implementation

Having gathered the data of phase, we moved toward the software side of our project. There are two major parts in the software setup. First is the reconstruction of vibration signal, and second is the measurement of vibrational period.

5.1 Reconstructing Vibration Signal

5.1.1 Compressive Sensing:

Compressive sensing is a signal processing technique to recover the sparse signal from the non-uniformly sampled points through solving the L1 optimization problem [31], [32]. Since our vibration signal is a periodic signal, it has finite number of non-zero frequency components. This means that our desired signal has sparse representation in the frequency domain. Moreover, the non-uniform sampling by the RFID reader introduces randomness in the samples. Kolmogorov-Smirnov test (KS-test) applied on the received data from the reader also verified that the read time of the reader follows the uniform distribution [20]. After ensuring that our data satisfies both conditions of sparseness and randomness, we use the technique of compressive sensing to recover the vibration signal.

5.1.1.1 Problem Formulation:

Let $s[n]$ is our desired vibration signal where $n = 1, 2, \dots, N$.

$$S[k] = \sum_{n=1}^N s[n] e^{\frac{-j2\pi(k-1)(n-1)}{N}}$$

$S[k]$ is the discrete Fourier transform of $s[n]$, where $k = 1, 2, \dots, N$. We can transform the $s[n]$ into its sparse discrete Fourier transform 'S' with Ψ as follows:

$$S = \Psi s$$

Where Ψ is the $N \times N$ matrix contain Fourier basis, $\Psi[i, j] = e^{-j2\pi i(i-1)(j-1)/N}$ for $i, j = 1, 2, \dots, N$, 's' is the vibration signal containing N points, and 'S' is the 'N' dimensional coefficient vector.

The next step is to construct the Measurement Martix Φ . The matrix phi is $M \times N$ matrix containing only 1s and 0s. where $M = \lceil N/Q \rceil$. 'Q' is a hyperparameter controlling the size of a reading frame. Each entry in a measurement matrix is considered as a reading slot. Then reading frame is made by aggregating the 'Q' reading slots. Each row of matrix Φ contains only one read frame. So, there are total of $M = \lceil N/Q \rceil$ read frames. The m th readframe is in the m th row starts from the $((m-1)Q + 1)$ th reading slot and ends at the mQ th reading slot. $\Phi[m, n] = 1$, if tag was read at n th reading slot, and $\Phi[m, n] = 0$, if tag was not read at the n th reading slot. Let Y is $M \times 1$ vector, where $Y[m]$ is just the aggregate of the values read in m th reading frame.

$$Y[m] = \sum_{n=1}^N \Phi[m, n]s[n]$$

We can write the measurement model with the consideration of a measurement noise 'n' as

$$Y = \Phi s + n$$

The overall model becomes

$$Y = \Phi \Psi^{-1} S + n$$

The 'S' is the sparse representation of desired signal 's', which has 'K' non-zero elements. The number of non-zero elements and their positions in the 'S' is unknown. If we recover this 'S' vector then we can simply get the desired signal 's' through inverse Fourier Transform. Compressive sensing tells that we can recover this sparse 'S' vector by solving the L1 optimization problem [32].

$$\begin{aligned} \hat{S} &= \min_S \|S\|_1 \\ \text{s.t. } &\|y - \Phi \Psi^{-1} S\|_2 \leq \epsilon \end{aligned}$$

where ϵ is the small predefined error threshold. We can find the solution to this

L1 optimization problem by using the techniques of linear programming [32]. In order to get the time domain representation of our reconstructed signal 's', we take the inverse Fourier transform of the recovered 'S'.

$$s = \Psi^{-1}S$$

Compressive sensing adds a constraint on the 'M', which is the size of the measurements we use to recover our vibrational signal. If $M > bu^2(\Phi, \Psi)K \log[N]$, only then compressive sensing able to recover the signal [33]. Where 'b' is positive constant, $u^2(\Phi, \Psi)$ is a coherence between measurement matrix Φ , and representation basis Ψ . The coherence metric is the largest correlation between any two elements of the Φ and Ψ .

$$u(\Phi, \Psi) = \sqrt{N} \max_{1 \leq i, j \leq N} | \langle \Phi_i, \Psi_j \rangle |$$

Due to the inherent randomness in reading time of the RFID reader, the measurement matrix Φ becomes random. Due to the randomness in matrix Φ , it is largely incoherent with any fixed representation basis Ψ . Hence, the above condition is satisfied. Usually M of the order of $3K \sim 4K$ is sufficient for good reconstruction.

5.1.1.2 Implementation:

We have implemented the above-mentioned algorithm in MATLAB. To check the validity of this reconstruction algorithm, we performed various simulations in MATLAB in which we generated the data in MATLAB, so that we had the ground truth of the desired signal 's'. To emulate the phase readings from the reader that have some measurement noise and are non-uniformly sampled, we applied the Additive White Gaussian Noise (AWGN) to our synthetic signal, and then randomly sampled some points of the data. After that we tried to recover the desired signal s through the implemented algorithm from this randomly sampled noisy data. As a metric of performance, we used the sum of the squared error of each recovered point from the original point.

$$E = \frac{\|s - r\|_2}{\|s\|_2}$$

This metric makes sense because it is just a normalized sum of the square of the Euclidean distance of each recovered point from its actual location. The farther the recovered point is from its actual location, the more error is caused by that point. The error becomes lesser and lesser as the recovered points starts moving

toward their actual point, and eventually becomes zero when the recovered signal is exactly equals to the actual signal.

Experiments are performed with various periodic signals. The algorithm shows the promising results. Two of the simulation results are attached below:

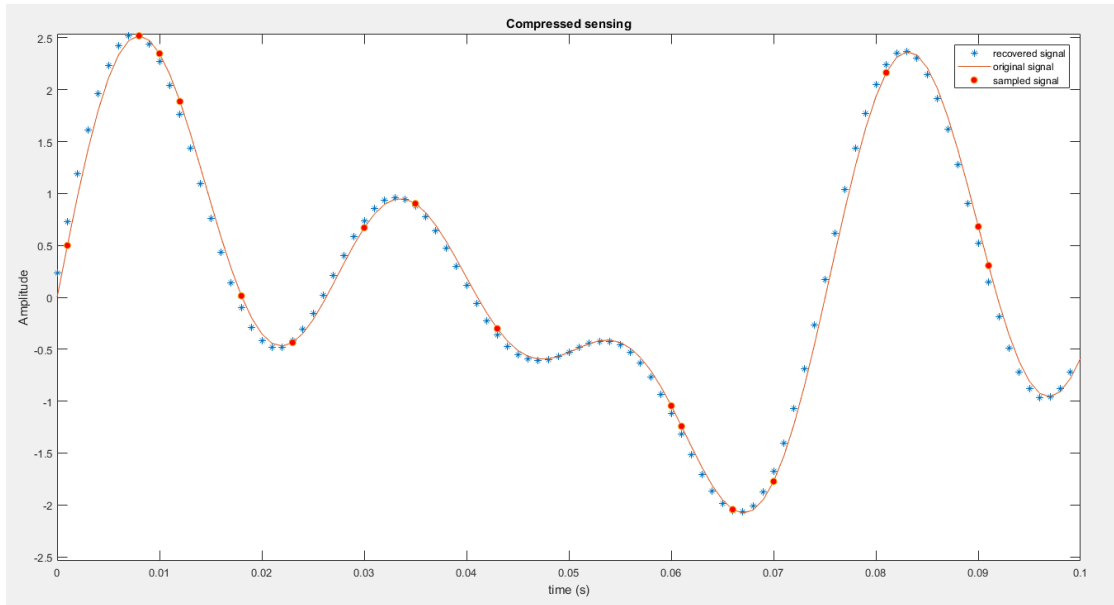


FIGURE 5.1: Reconstructed signal 1

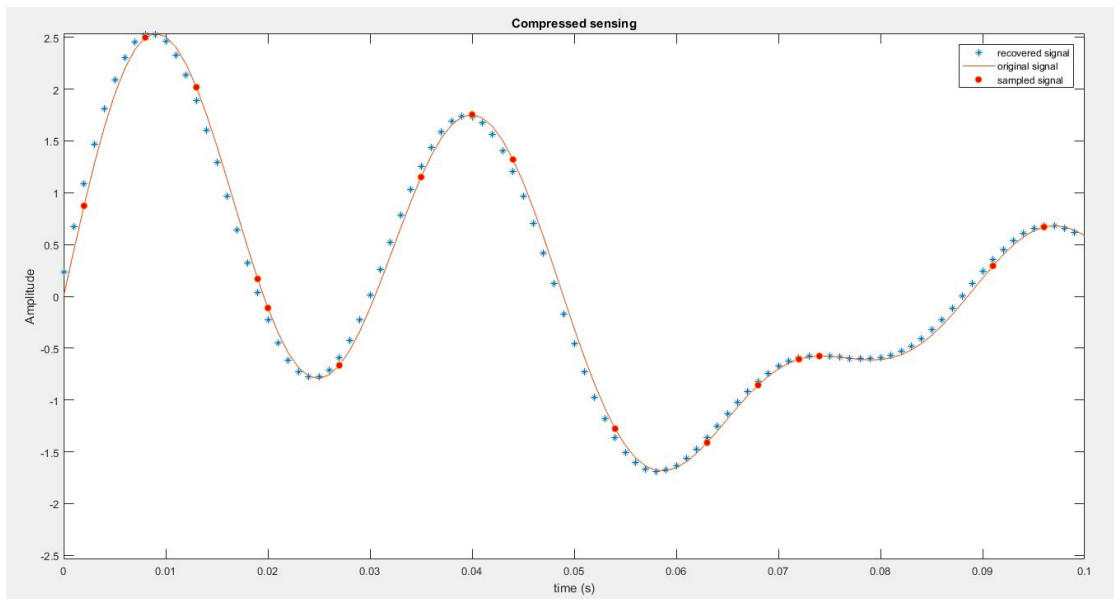


FIGURE 5.2: Reconstructed signal 2

In Fig5.1 and Fig5.2, line shows the synthetic periodic signal, orange colored dots represents the randomly sampled points, and the '*' shows the reconstructed signal from the randomly sampled points. You can see that algorithm is able to

completely recover the trend the desired signal even if the given number of sample points are too less and non-uniform spaced.

5.1.1.3 Effect of Noise on recovery:

To get an idea of the effect of the measurement noise on the error of our algorithm, we performed the experiment for different noise levels and plotted the graph shown in Fig5.3. The graph depicts that the noise has a great effect on the recovery error. The error increases exponentially when SNR decreases below 20 dB. But the recovery error is somewhat negligible for SNR greater than 20 dB. It makes sense because when SNR is low, it adds the frequency components other than the frequency components of the vibration signal. The signal no longer remains sparse in the frequency domain because of which compressive sensing is unable to recover the signal because sparsity is the requirement of this recovery algorithm.

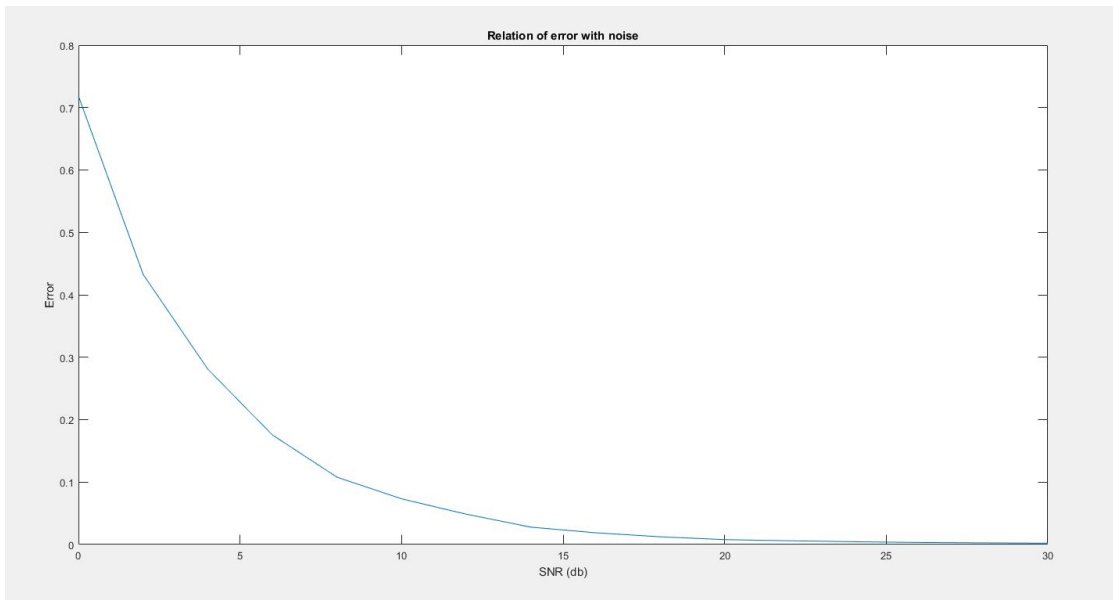


FIGURE 5.3: Effect of noise on error

5.2 Measuring Vibrational Period

5.2.1 Fourier Transform:

One way to measure the vibrational period T_s is through the Fourier Transform. Fourier Transform of the vibration signal tells which frequency components are present in the vibration signal. The minimum frequency f_{min} component that is present in the Fourier Transform is the vibrational frequency f_s . Then vibrational period turns out to be the inverse of vibrational frequency.

$$f_s = f_{min}$$

$$T_s = f_s^{-1}$$

But there are some issues in this approach. Fourier Transform is very sensitive to the noise. Minute noise can add frequency components in the Fourier domain, and change the position of the frequency components. The data received from the reader has an inherent measurement noise, and then we reconstruct the signal through compressive sensing which may have some estimation error. So the computation of vibration period T_s from this approach of Fourier Transform is less likely to give the correct period.

5.2.2 Finding Time Period Through Correlation Method:

This approach measures the vibrational period of the periodic signal by computing the correlation of vibration signal for different values of the lag (delay).

$$Correlation = A[l] = \sum_{n=1}^N s_1[n]s_2^*[n-l]$$

Since our signal $s[n]$ is real valued signal so conjugate $s_2^*[n] = s_2[n]$. where 'l' is the lag.

Intuition behind this approach is that correlation is the measure of similarity between two signals. So, correlation is maximum when $s_1[n] = s_2[n] = s[n]$. So we compute correlation with $s_1[n] = s[n]$ and $s_2[n] = s[n-l]$ for $l = 0, 1, 2, \dots, N-1$. This gives us the correlation signal $A[l]$. Let L is the period of our vibration signal $s[n]$, which means

$$s[n] = s[n-L]$$

We first compute the correlation when $l=0$, then start increasing l . We again see a spike in correlation when $l = L$, because at this point $s[n]$ is shifted by exactly one period and the $s_2[n]$ becomes equal to $s[n]$ again. Because of this periodicity we see spikes in correlation at all integer multiples of time period L . We ignore the peak at $l = 0$, because it is just the autocorrelation of a signal. We use the lag value of the first peak after $l = 0$ to compute the vibrational period because it gives the shortest time at which signal starts to repeat itself which is the fundamental period of the periodic signal.

We performed an experiment in MATLAB with a synthetic periodic signal with the periodic frequency of 15 Hz (Time period 0.667 sec) and computed its correlation for different values of lag. We compared the lag value of the first peak in correlation after the zero lag with the actual time period, and it turned out to be the same (0.667 sec). The Fig5.4 shows the graph of correlation with respect to the lag.

The cursor on the graph clearly shows the location of the first peak after zero lag is 0.66 sec.

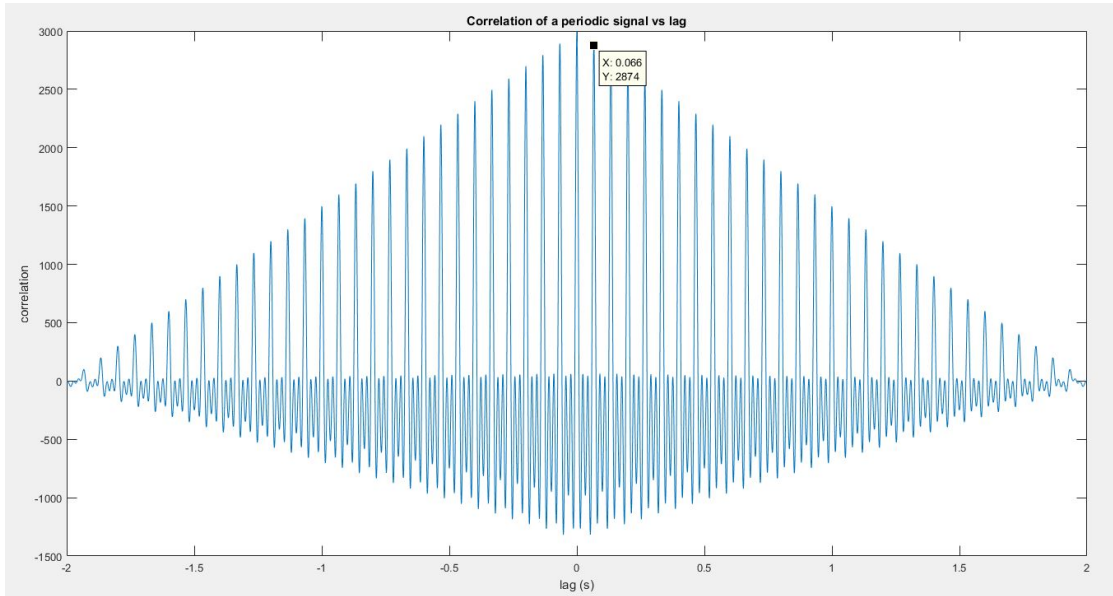


FIGURE 5.4: The correlation of a periodic signal with respect to lag

5.3 Experimentation

After performing extensive simulations of reconstructing vibration signal through compressive sensing and finding the fundamental period of periodic signal using correlation method on MATLAB, we moved toward measuring the RPM of different rotary machines. For the ground truth, we measured the RPM with the help of tachometer. Our experimental setup is that we pasted a tag on the rotatory part of the machine, and placed circular polarized antenna of the reader in front of the tag at approximately a distance of 1 meter. Then rotary machine was set to rotate at a fixed RPM. After this hardware setup, reader started to collect phase values along with their timestamps and stored them in a file with the help of LLRP toolkit. These phase values with their time stamps were then passed to MATLAB where our implemented algorithm first reconstructed the vibration signal through the compressive sensing algorithm, and then measured the vibration period with the help of correlation method.

We performed experiments on an induction motor at various different RPMs, and on a pedestal fan at three different RPMs. We performed 10 experiments at each RPM. Each experiment collected the data for 5 seconds. Some of our experimentation results are shown below:

The Fig5.5, 5.6, and 5.7 are the results of the experiments on an induction motor.

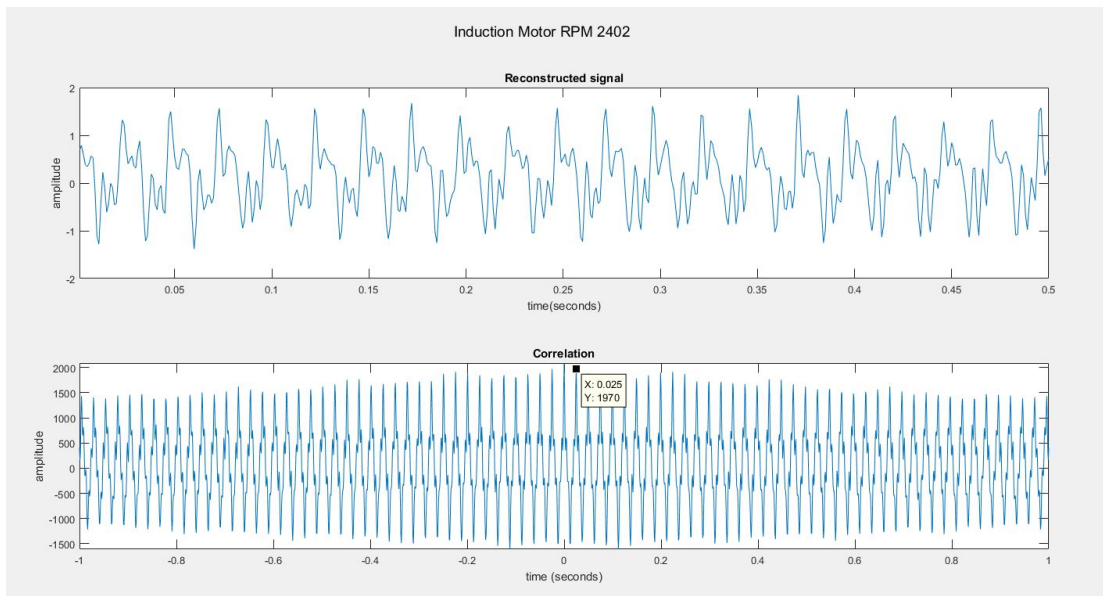


FIGURE 5.5: The reconstructed vibration signal of an induction motor rotating at 2402 RPM and its correlation with respect to lag

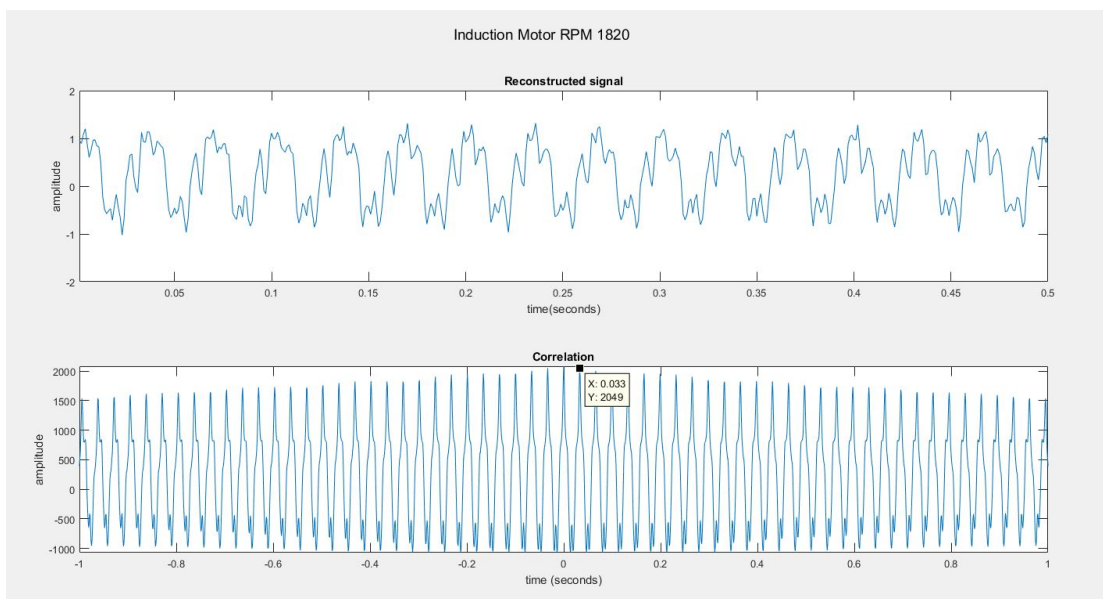


FIGURE 5.6: The reconstructed vibration signal of an induction motor rotating at 1820 RPM and its correlation with respect to lag

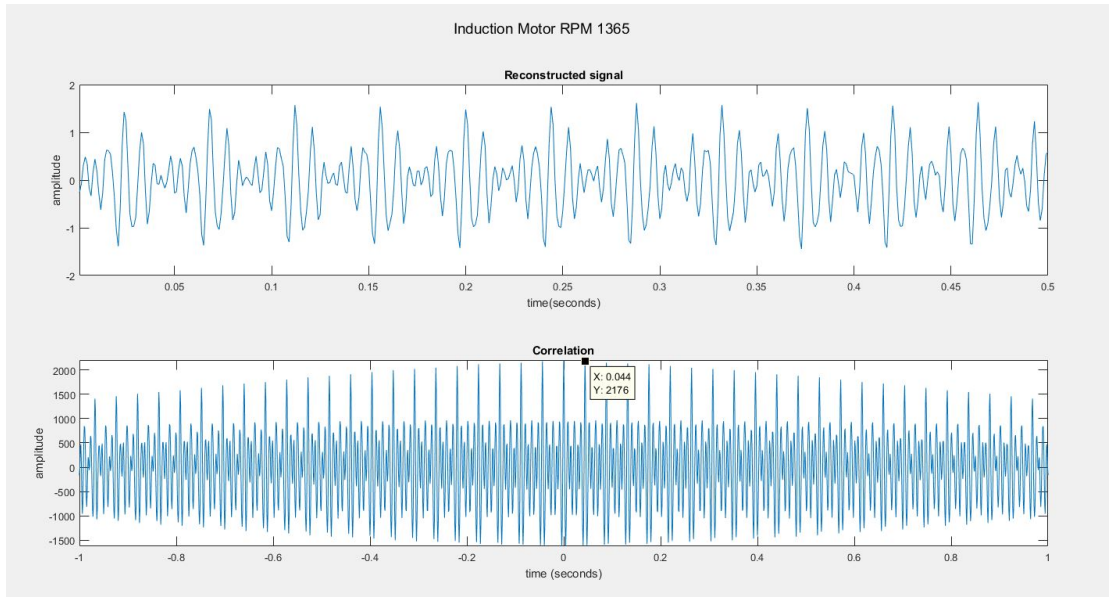


FIGURE 5.7: The reconstructed vibration signal of an induction motor rotating at 1365 RPM and its correlation with respect to lag

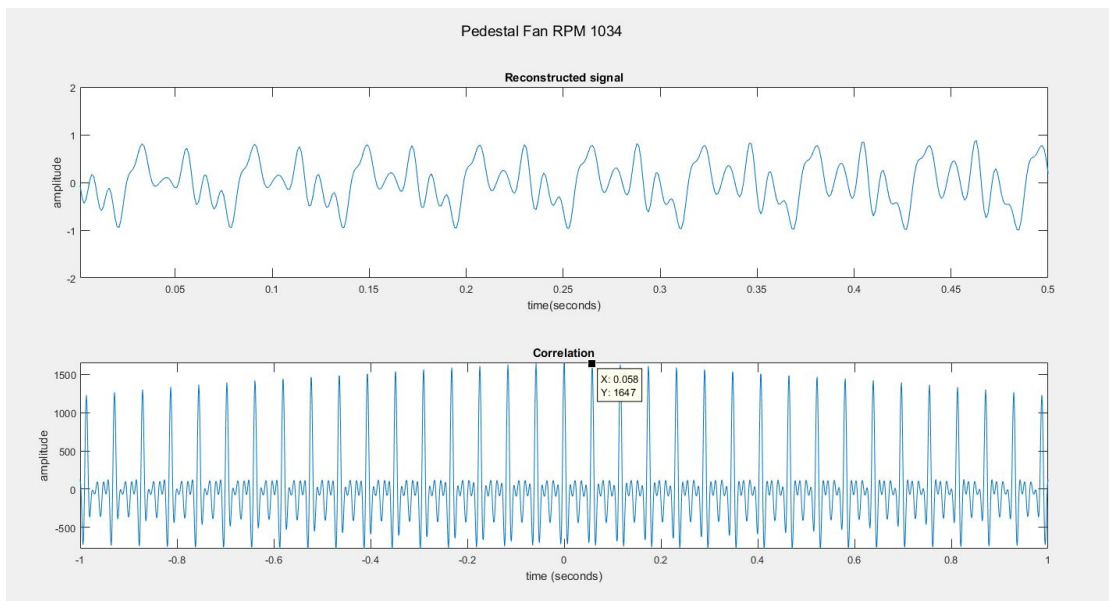


FIGURE 5.8: The reconstructed vibration signal of an pedestal fan rotating at 1034 RPM and its correlation with respect to lag

Each figure contains 2 subplots. Subplot 1 in Fig5.5, 5.6, and 5.7 displays the reconstructed signal by compressive sensing when induction motor revolving at 2402 RPM, 1820 RPM, and 1365 RPM respectively. Subplot 2 in each figure shows the correlation of their reconstructed signal with respect to lag. The cursor is placed on each figure at the first peak after the zero lag, which gives us the lag value which is the fundamental period T_s of their signals. Then we can compute RPM by $60/T$. Subplot 2 Fig5.5, 5.6, and 5.7 gives time period 0.025s (2402 RPM),

0.033s (1802 RPM), and 0.044s (1365 RPM) respectively.

The Fig5.5 is the result of the experimentation on a pedestal fan at 1034 RPM. Subplot 1 shows the reconstructed vibration signal of a pedestal fan. Subplot 2 is the correlation of a reconstructed signal with respect to the lag. First peak of correlation after zero lag is at 0.058 second shown by cursor as well. The time period of 0.058 is equal to 1034 RPM.

5.4 Error Analysis

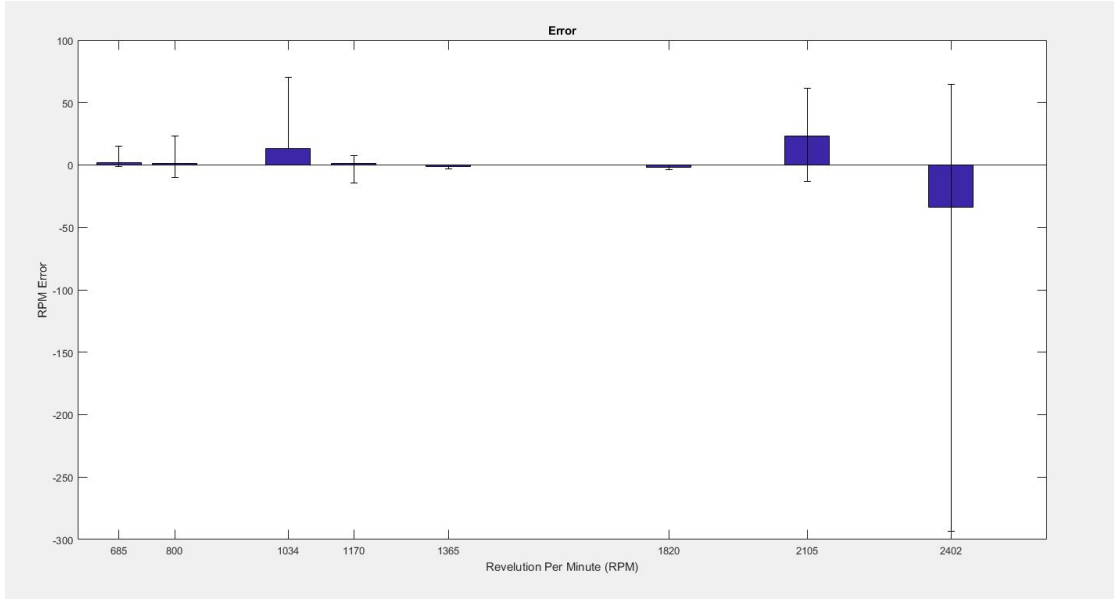


FIGURE 5.9: The mean, minimum, and maximum error in a measurement with respect to the corresponding RPMs

In the experimentation step, we have performed 10 experiments at each RPM. Then we computed the error:

$$Error = RPM_{measured} - RPM_{groundtruth}$$

Where $Error$ is a vector of size 10, because we performed 10 experiments for each RPM. Then we plot a graph shown in Fig5.9 where x-axis corresponds to the RPM of a machine at which experiment was conducted, and y-axis corresponds to the error in RPM measurement. The blue shaded region shows the mean error, lowest peak shows the minimum value in error, and highest peak shows maximum value in error we got during the experiment at the corresponding RPM at x-axis.

It is clear from the graphs that the mean error is quite low which means that our system is able to measure the RPM of machine just by tagging the machine and getting the phase values through the reader.

Chapter 6

Conclusion, Future Recommendations, And Cost Analysis

6.1 Conclusion and Future Recommendations

Having successfully measured the RPM of a rotatory motion, the obvious next step is to extend the experimentation to vibration analysis. Throughout our project, we have not assumed the motion to be necessarily rotatory, we only assumed the periodicity of the signal. Since vibration signal is also periodic in nature, our project should smoothly extend to linear vibration. However, one thing that needs to be considered is that the amplitude of the vibration signal is relatively small compare to a rotatory motion. Moreover, the time period of many vibration signal is smaller in comparison to a rotatory motion. Hence, the sampling rate of COTS RFID reader and the frequency at which it operates - 866 MHz - might act as a bottleneck in our analysis. This is because the frequency of the operation determines the amplitude we can sense, and the sampling rate will limit the frequency of the vibration that we can detect. Therefore, it is essential to find an alternate to COTS RFID reader so that we can work around these apparent limitations.

One way to overcome these limitations and to extend our analysis is to use universal software radio peripheral (USRP). There is an existing implementation of Gen2 UHF RFID reader with USRP and GNU Radio at [34]. This implementation can be extended to extract the phase using the preamble correlation. An obvious advantage of a USRP implementation is the ability to change the central frequency of communication. Since the EPC class 1 Gen2 protocol is valid in the frequency band of 860 – 930 MHz, so we can operate the experimental part of our project at

higher frequency compare to 866 MHz of the COTS RFID reader. Hence, we can sense the vibration of a smaller amplitude. Moreover, the USRP implementation offers a higher sampling rate which allows the phase sampling at a higher rate. Moreover, there is no ambiguity of ' π ' radians in the phase values calculated from the USRP, which is a limitation of commercial readers.

6.2 Cost Analysis

The table 6.1 shows the cost of the equipment involved in our project. Despite this seemingly high initial cost, note that this application is aimed to reduce industrial machinery downtime and allow for the possibility of maintenance before things get catastrophic. Hence, in its application it will save an industry several folds more than the cost to implement this system. Thus, making this as one of the most effective scheme.

TABLE 6.1: Cost Analysis

| Sr.no | Description | QTY | Unit Price (USD) | Total (USD) |
|-------|--|-----|------------------|-------------|
| 1 | IMPINJ R420 Reader (IPJ-REV-R420-EU12M1) | 1 | 1189 | 1189 |
| 2 | AC power cord (IPJA2051) | 1 | 20 | 20 |
| 3 | AC power Supply (IPJA2003-000) | 1 | 59 | 59 |
| 4 | Perfect Wave Antenna (flush mount) | 4 | 143 | 572 |
| 5 | RF Cables for Antenna (1 meter) | 2 | 3 | 6 |
| 6 | RF Cables for Antenna (2 meter) | 2 | 6 | 12 |
| 7 | Speedway Connect Software License | 1 | 175 | 175 |
| 8 | sample tags (including metal label) | 1 | 15 | 15 |
| 9 | - | - | - | 2048 |

References

- [1] P. Nikitin and K. Rao. (2007, 01) Theory and measurement of backscattering from rfid tags.
- [2] M. Buettner and D. Wetherall, “A flexible software radio transceiver for uhf rfid experimentation: Uw tr: Uw-cse-09-10-02,” 04 2011.
- [3] R. Arsenault. (2016) Stat of the week: The (rising!) cost of downtime. [Online]. Available: <https://www.aberdeen.com/techpro-essentials/stat-of-the-week-the-rising-cost-of-downtime/>
- [4] R. Valluri. (2018) What is the problem industry is facing with machine’s maintenance? [Online]. Available: <https://minto.ai/2018/07/17/why-iiot-series1/>
- [5] M. Homer. [Online]. Available: <http://fieldservicenews.com/author/mark-homer/>
- [6] V. B. R. Study. After the fall: Cost, causes and consequences of unplanned downtime. [Online]. Available: <https://lp.servicemax.com/Vanson-Bourne-Whitepaper-Unplanned-Downtime-LP.html>
- [7] D. Galar and U. Kumar, *eMaintenance: Essential Electronic Tools for Efficiency*, 01 2017.
- [8] S. Edwards, A. Lees, and M. Friswell, “Fault diagnosis of rotating machinery,” *The Shock and Vibration Digest*, vol. 30, pp. 4–13, 01 1998.
- [9] C. Yung. (2006, Jun) Vibration analysis: what does it mean? [Online]. Available: <https://www.plantservices.com/articles/2006/154/>
- [10] Atin. (2019, Sep) Importance of overall vibration measurements in predictive maintenance. [Online]. Available: <http://www.sensegrow.com/blog/overall-vibration-measurements-iiot-predictive-maintenance>

- [11] C. Fayad. (2014) Using integrated control and asset management to optimize maintenance and reliability. [Online]. Available: <https://www.flowcontrolnetwork.com/using-integrated-control-asset-management-to-optimize-maintenance-reliability/>
- [12] Condition based maintenance & monitoring (cbm maintenance). [Online]. Available: <https://www.fixsoftware.com/condition-based-maintenance/>
- [13] J. Sobral and C. Guedes Soares, “Preventive maintenance of critical assets based on degradation mechanisms and failure forecast,” *IFAC-PapersOnLine*, vol. 49, 12 2016.
- [14] K. Hagerty. (2019, Nov) How condition-based maintenance helps predict and prevent unplanned downtime. [Online]. Available: <https://www.prescriptivedata.io/content/chart-of-the-day/ibm-iot-how-condition-based-maintenance-helps-predict-and-prevent-unplanned-downtime>
- [15] M. Lenehan. (2017) Speedway antenna hub product brief. [Online]. Available: <https://support.impinj.com/hc/en-us/articles/202755698-Speedway-Antenna-Hub-Product-Brief-Datasheet>
- [16] Epc uhf gen2 air interface protocol. [Online]. Available: <http://www.gs1.org/epcrfid/epc-rfid-uhf-air-interface-protocol/2-0-1>.
- [17] “Epc radio-frequency identity protocols, class-1 generation-2 uhf rfid protocol for communications at 860 mhz-960 mhz, version 2.0.1. epc global,,” 2015.
- [18] N. Kargas, F. Mavromatis, and A. Bletsas, “Fully-coherent reader with commodity sdr for gen2 fm0 and computational rfid,” *IEEE Wireless Communications Letters*, vol. 4, pp. 1–1, 12 2015.
- [19] EPCglobal. (2010) Low level reader protocol llrp. [Online]. Available: <https://www.gs1.org/standards/epc-rfid/llrp/1-1-0>
- [20] L. Yang, Y. Li, Q. Lin, X. Li, and Y. Liu, “Making sense of mechanical vibration period with sub-millisecond accuracy using backscatter signals,” 10 2016, pp. 16–28.
- [21] C. Duan, L. Yang, H. Jia, Q. Lin, Y. Liu, and L. Xie, “Robust spinning sensing with dual-rfid-tags in noisy settings,” 04 2018, pp. 855–863.
- [22] (2018) Lion precision. [Online]. Available: <http://www.lionprecision.com/>

- [23] S. Seitz and C. Dyer, “View-invariant analysis of cyclic motion,” *International Journal of Computer Vision*, vol. 25, 01 1997.
- [24] N. Pontius. (2020, Feb) What are rfid tags? learn how rfid tags work, what they’re used for, and some of the disadvantages of rfid technology. [Online]. Available: <https://www.camcode.com/asset-tags/what-are-rfid-tags/>
- [25] Epc gen2 commands for rfid readers. [Online]. Available: <https://rfid4u.com/rfid-basics-resources/epc-gen2-reader-commands-and-q-parameter/>
- [26] M. Lenehan. Ltk libraries for impinj speedway rain rfid readers. [Online]. Available: <https://support.impinj.com/hc/en-us/articles/202755488-LTK-Libraries-for-Impinj-Speedway-RAIN-RFID-readers>
- [27] ——. Hello llrp (low-level reader protocol). [Online]. Available: <https://support.impinj.com/hc/en-us/articles/202756168-Hello-LLRP-Low-Level-Reader-Protocol->
- [28] ——. (2020, Jan) Get low-level reader data with llrp. [Online]. Available: <https://support.impinj.com/hc/en-us/articles/202756348-Get-Low-Level-Reader-Data-with-LLRP>
- [29] ——. Low level user data support. [Online]. Available: <https://support.impinj.com/hc/en-us/articles/202755318-Application-Note-Low-Level-User-Data-Support>
- [30] ——. (2020, Feb) Understanding epc gen2 search modes and sessions. [Online]. Available: <https://support.impinj.com/hc/en-us/articles/202756158-Understanding-EPC-Gen2-Search-Modes-and-Sessions>
- [31] D. Donoho, “For most large underdetermined systems of linear equations the minimal l_1 -norm solution is also the sparsest solution,” *Comm. Pure Appl. Math*, vol. 59, 01 2006.
- [32] ——, “Compressed sensing,” *IEEE Transactions on Information Theory*, vol. 52, pp. 1289–1306, 01 2006.
- [33] E. Candès, J. Romberg, and T. Tao, “Robust uncertainty principles : Exact signal frequency information,” *Information Theory, IEEE Transactions on*, vol. 52, pp. 489–509, 03 2006.
- [34] N. Kargas, F. Mavromatis, and A. Bletsas, “Fully-coherent reader with commodity sdr for gen2 fm0 and computational rfid,” *IEEE Wireless Communications Letters*, vol. 4, pp. 1–1, 12 2015.